

Analysis of Volume Fraction and Convective Heat Transfer on MHD Casson Nanofluid over a Vertical Plate

John Kinyanjui Kigio, Mutuku Winifred Nduku, Oke Abayomi Samuel*

Department of Mathematics and Actuarial Science, Kenyatta University, Nairobi, Kenya

Email address:

okeabayomisamuel@gmail.com (O. A. Samuel)

*Corresponding author

To cite this article:

John Kinyanjui Kigio, Mutuku Winifred Nduku, Oke Abayomi Samuel. Analysis of Volume Fraction and Convective Heat Transfer on MHD Casson Nanofluid over a Vertical Plate. *Fluid Mechanics*. Vol. 7, No. 1, 2021, pp. 1-8. doi: 10.11648/j.fm.20210701.11

Received: February 27, 2021; **Accepted:** March 11, 2021; **Published:** May 8, 2021

Abstract: The numerous industrial and engineering applications of Casson nanofluid is due to the superiority of its thermophysical properties. Tomatoes paste, engine oil, soup etc., are examples of Casson fluid and when nanometer-sized particles are suspended in such Casson fluid, it becomes Casson nanofluid. This paper considers a natural convective magnetohydrodynamics flow of Cu-engine oil nanofluid across a convectively heated vertical plate. The effects of self-heating of the fluid (measured by the Eckert number), internal conductive resistance to external convective resistance (measured by the Biot number), magnetic field strength, volume fraction of the nanoparticles on the temperature and velocity of mass and heat transfer of Casson nanofluid is analysed. An appropriate model governing the flow of Casson nanofluid is formulated as a system of nonlinear partial differential equations. The natural convection boundary condition is included. To solve the problem, an appropriate similarity transformation is used to reformulate the system as a system of nonlinear ordinary differential equations. The shooting technique is used to convert the boundary problem to initial value problems before Runge-Kutta method, with the Gills constants, is used to solve the reformulated problem. The results are depicted as graphs. Flow velocity is found to increase as the base fluid becomes more Casson and as nanoparticle volume fraction increases. It is also found that increasing Eckert number, Biot number and magnetic field strength causes an increase in the flow temperature.

Keywords: Magnetohydrodynamics, Casson Fluid, Nanofluid, Convective Flow

1. Introduction

Heat transfer describes the flow of thermal energy due to temperature differences. The second law of thermodynamics establishes that heat flows from a region of higher temperature to a region of lower temperature unless the process is artificially conditioned. Heat transfer occurs only in three modes; conduction, convection, and radiation. Convection occurs when the temperature of the surface differs from that of the surrounding fluid. Convective heat transfer is one of the most natural phenomenon observed in fluid flow and this has attracted attention over the years. Several studies have been carried out to unravel the effect of natural convection on flow properties and some have even extended the researches to forced convection. It was also realised that extent of the influence of convective heat transfer in a flow depends largely on the nature of the fluid under consideration. Yang et al. [31]

studied convective heat transfer across a cylinder and found that the more the distance between the cylinder and the wall, the higher the heat transfer rate and drag force. Chen et al. [4] studied heat transfer in melting processes in an elliptical tube and a semi-analytical solution was obtained. The solution revealed that the melting rate increases with time. A further leap was taken by Kumar et al. [13] when the finite element method (FEM) was used to solve the Darcian flow with convection in an isothermal sinusoidal surface. This study ensured that the limitation of the finite element method was taken care of by avoiding restrictions on the geometrical nonlinearity arising from the parameters. The study revealed that there is an insignificant increase in the heat transfer rate when flow geometry moves from slender to blunt. Independently but simultaneously, Zerroukat et al. [32] adopted the collocation method with some radial basis functions to study heat transfer in different geometries while Piechowski [24] used experimental results to validate ground heat exchanger model

and carried out sensitivity analysis. Saadatian *et al.* [26] solved the 2D Darcy- Boussinesq equations using finite difference code over fine grid and it was found out that the heat transfer rate from the slender geometry is greater than that obtained in the blunt case in all cases. Kolenko *et al.* [10] analysed total radiative heat transfer in a furnace chamber.

The invention of electromagnetism by Hannes Alfvén (1908-1995) birthed the area of fluid dynamics called magnetohydrodynamics (MHD). MHD is the study of magnetic properties in electrically conducting fluids, such as plasmas, liquid metals, saltwater, and electrolytes. The result of the interaction between an electrically conducting fluid and a magnetic field plays a critical role in a variety of areas such as magnetic drug targeting, blood flow-meter, magnetic devices for cell separation, magnetohydrodynamic flow pump, treatment of cancer tumour, etc. Mutuku-Njane and Makinde [18] investigated an MHD nanofluid flow over a convectively heated vertical porous plate. The results indicated that an increase in the magnetic field strength and nanoparticle volume fraction has retarding effects on velocity profiles but enhance temperature profiles. Ahmad *et al.* [1] modified the work of Mutuku-Njane and Makinde [18] to consider MHD flow towards an exponentially stretching sheet in a porous medium and in the presence of radiation effects and Darcy's resistance. The study obtained an analytical solution using the Homotopy Analysis Method (HAM) and showed that thermal boundary layer thickness decreases with increasing Prandtl number. Ahmad *et al.* [2] studied MHD flow with the presence of internal heat source and a numerical investigation indicated that the heat transfer can be reinforced by increasing Prandtl number. In fact, it was observed that increasing thermal slip retards the flow temperature. Farooq *et al.* [5] decided to consider nanofluid whose base fluid is the electrically conducting Maxwell fluid. Investigation of the MHD flow showed that the Lorentz force induced by the magnetic field enhances the temperature and concentration of the flow. Recently, MHD flow of nanofluid was carried out with Cattaneo-Christov heat flux model [28], over corrugated vibrating bottom surface [8] while some semi-analytical approaches to solving the equations were presented by Bulinda *et al.* [3]. Each of these studies observes that temperature is enhanced with increasing magnetic force.

The enhanced physical and thermal properties of the nanofluid make it very applicable in cooling processes, refrigerators, laptops etc. Many of the recent researches in fluid mechanics are on nanofluid flows. By taking the Casson fluid as the base fluid, the Casson nanofluid is birthed. The Casson nanofluid is of far-reaching impact in emulsion companies, bioreactors, medical engineering etc. A more robust fluid flow is birthed when the powerful effect of convective boundary heating is included in the flow of Casson nanofluid under the influence of magnetic field. The results of this research shall provide more useful hints specifically to industries involved in thermocooling, vehicular fluid, magnetic drug targeting, geothermal reservoirs, heat exchangers, ablation, medical sciences, metallurgy etc. Nadeem *et al.* [19] investigated the Casson fluid flow past a

porous linearly stretching sheet and observed that flow resistance increases with an increasing Casson parameter and magnetic field strength. The skin-friction coefficient in the x -direction increased with an increase in the stretching ratio. The coefficient of skin friction increases with increasing magnetic field strength. Meanwhile, Pramanik [25] analysed heat transfer in Casson fluid flow on an exponentially porous stretching surface and observed that increasing Casson fluid parameter suppresses the velocity but enhances temperature. The outcome corroborates the earlier results of previous studies [18, 19]. The effects of variable thermal conductivity on Casson fluid flow was also examined by Idowu *et al.* [7] by studying the effects of a non-Darcian porous medium, nonlinear radiation as well as temperature-dependent thermal conductivity and viscosity on Casson flow. Mahantesh *et al.* [14] modified [7] to include the presence of non-linear thermal radiation while the flow is over a moving vertical plate.

Mustafa and Khan [16] modified [25] by extending the flow to Casson nanofluid under the influence of magnetic field and the result was still in full agreement with earlier results. The fact that the effectiveness of automotive radiators is directly related to the type of fluid used in their preparation motivated Mutuku [17] to consider Ethylene-Glycol-based nanofluid. The results also agree with the existing results. A further extension was done by Kataria and Patel [9] to consider an oscillating vertical plate. An analytic solution was obtained using the Laplace Transform and expressions were obtained for the dimensionless velocity and temperature. The work of Idowu *et al.* [7] was extended by Gbadeyan *et al.* [6] to Casson nanofluid to examine the effects of a non-Darcian porous medium, nonlinear radiation as well as temperature-dependent thermal conductivity and viscosity on Casson nanofluid flow. Shah *et al.* [27] also extended the work of Mahantesh *et al.* [14] to Casson nanofluid. Other recent works on Casson fluid, nanofluid and magnetohydrodynamic flows include [11, 12, 20-22].

Despite the rapt attention of researchers to the superiority of the thermophysical properties of the nanofluid over the base fluid and the macrosized particles, and from the aforementioned literature, it is clear that no one has considered convective magnetohydrodynamics flow of Casson nanofluid over a convectively heated surface. This study is motivated to address this research gap. A natural convective heat transfer in magnetohydrodynamic flow of Casson nanofluid over a convectively heated stretching vertical surface is analysed in this study.

2. Governing Equations

A nanofluid whose base fluid is the Casson fluid is considered to flow across a vertical plate as shown in figure 1. A magnetic field of strength B_0 is applied normal to the flow. The surface is subjected to a convective heating boundary condition.

Equations governing the natural convective flow of electrically conducting Casson nanofluid under the influence of magnetic field are given in equations (1-4).

$$\frac{\partial u}{\partial x} + \frac{\partial v}{\partial y} = 0, \quad (1)$$

$$u \frac{\partial u}{\partial x} + v \frac{\partial u}{\partial y} = \frac{\mu_{nf}}{\rho_{nf}} \left(1 + \frac{1}{\gamma}\right) \frac{\partial^2 u}{\partial y^2} + g\beta_T(T - T_\infty) + g\beta_C(C - C_\infty) - \frac{\sigma_{nf} B_0^2 u}{\rho_{nf}}, \quad (2)$$

$$u \frac{\partial T}{\partial x} + v \frac{\partial T}{\partial y} = \alpha_{nf} \frac{\partial^2 T}{\partial y^2} + \tau \left(D_B \frac{\partial C}{\partial y} \frac{\partial T}{\partial y} + \frac{D_T}{T_\infty} \left(\frac{\partial T}{\partial y} \right)^2 \right) + \frac{\mu_{nf}}{(\rho c_p)_{nf}} \left(\frac{\partial u}{\partial y} \right)^2 + \frac{\sigma_{nf} B_0^2 u^2}{(\rho c_p)_{nf}}, \quad (3)$$

$$u \frac{\partial C}{\partial x} + v \frac{\partial C}{\partial y} = D_B \frac{\partial^2 C}{\partial y^2} + \frac{D_T}{T_\infty} \frac{\partial^2 T}{\partial y^2}. \quad (4)$$

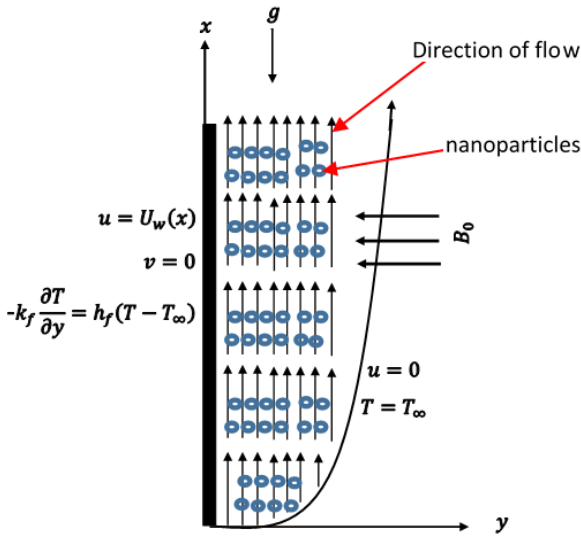


Figure 1. Flow schematic diagram.

subject to the boundary conditions at $y = 0$:

$$u = ax, v = 0, -k_f \frac{\partial T}{\partial y} = h_f(T_f - T), C = C_w(x), \quad (5)$$

as $y \rightarrow \infty$:

$$u \rightarrow 0, T \rightarrow T_\infty, C \rightarrow C_\infty, \quad (6)$$

where $\alpha_{nf} = \frac{\kappa_{nf}}{(\rho c_p)_{nf}}$, $\tau = \frac{(\rho c_p)_{np}}{(\rho c_p)_{bf}}$.

Using the models proposed by Maiga et al. [15], Pak and Cho [23], Wasp [29] and Xuan and Roetzel [30], the effective density, viscosity, specific heat capacity, and thermal conductivity of the nanofluid are given as

$$\frac{k_{nf}}{k_{bf}} = \frac{k_{np} + 2k_{np} - 2\phi(k_{bf} - k_{np})}{k_{np} + 2k_{bf} + \phi(k_{bf} - k_{np})}, \quad (7)$$

$$\rho_{nf} = (1 - \phi)\rho_{bf} + \phi\rho_{np}, \quad (8)$$

$$(\rho c_p)_{nf} = (1 - \phi)(\rho c_p)_{bf} + \phi(\rho c_p)_{np}, \quad (9)$$

$$\frac{\mu_{nf}}{\rho_{nf} \nu_{bf}} = \frac{0.904e^{0.148\phi}}{(1 - \phi + \phi \frac{\rho_{np}}{\rho_{bf}})}. \quad (10)$$

3. Methodology

The Solution of the governing system of nonlinear partial differential equations (1 - 6) is in three steps; nondimensionalisation by Similarity Transformation, solving using Runge-Kutta-Gills method in MATLAB bvp4c, and finally simulating the solution and depicting the solutions in graphs.

3.1. Nondimensionalisation of the Governing Equation

The governing partial differential equations are converted to ordinary differential equations using the similarity variables

$$\eta = y \sqrt{\frac{a}{\nu}}, u = \frac{\partial \psi}{\partial x}, v = -\frac{\partial \psi}{\partial y}, \quad (11)$$

$$T = T_\infty + (T_w - T_\infty)\theta, C = C_\infty + (C_w - C_\infty)\phi \quad (12)$$

from which the stream function is obtained as

$$\psi = \sqrt{a\nu}xf(\eta). \quad (13)$$

Consequently, to satisfy the continuity equation, we choose u and v as

$$u = axf', v = -\sqrt{a\nu}f(\eta). \quad (14)$$

From the ongoing, and setting the parameters as

$$Gr_t = \frac{g\beta(T_w - T_\infty)}{a^2 x}; Gr_s = \frac{g\beta^*(C_w - C_\infty)}{a^2 x}; Sc = \frac{\nu}{D_B};$$

$$Ec = \frac{a^2 x^2}{(C_p)_{nf}(T_w - T_\infty)}; Pr = \frac{\nu_{bf}}{\alpha_{bf}}; M = \frac{\sigma_{nf} B_0^2}{a\rho_{nf}};$$

$$N_b = \frac{\tau D_B}{\alpha_{bf}}; N_t = \frac{\tau D_T(T_w - T_\infty)}{\alpha_{bf} T_\infty}; Bi = \frac{h_f}{k_f} \sqrt{\frac{\nu}{a}};$$

$$A_1 = \frac{\left(\frac{k_{np} + 2k_{bf} - 2\phi(k_{bf} - k_{np})}{k_{np} + 2k_{bf} + \phi(k_{bf} - k_{np})} \right)}{\left((1 - \phi) + \phi \frac{(\rho c_p)_{np}}{(\rho c_p)_{bf}} \right)};$$

the dimensionless equations are

$$\frac{\mu_{nf}}{\rho_{nf} \nu_{bf}} \left(1 + \frac{1}{\gamma}\right) f'''' - f'f'' + ff'' + Gr_t \theta + Gr_s \phi - Mf' = 0, \quad (15)$$

$$A_1 \theta'' + Pr f \theta' + N_b \phi' \theta' + N_t (\theta')^2 + \frac{\mu_{nf}}{\rho_{nf} \nu_{bf}} Pr Ec (f'')^2 + Pr MEc (f')^2 = 0, \quad (16)$$

$$\Phi''' + Sc \Phi' f + \frac{N_t}{N_b} \theta'' = 0. \quad (17)$$

with the initial and boundary conditions at $\eta = 0$;

$$f(0) = 0; f'(0) = 1; \theta'(0) = -Bi(1 - \theta); \phi(0) = 0; \quad (18)$$

as $\eta \rightarrow \infty$;

$$f' \rightarrow 0; \theta \rightarrow 0; \phi \rightarrow 0. \quad (19)$$

To rewrite these equations as a system of first order

ordinary differential equations, we set

$$\begin{aligned} X_1 &= f, X_2 = f', X_3 = f'', X_4 = \theta, \\ X_5 &= \theta', X_6 = \Phi, X_7 = \Phi' \end{aligned} \quad (20)$$

So that the equations becomes

$$X'_1 = X_2, \quad (21)$$

$$X'_2 = X_3, \quad (22)$$

$$X'_3 = \frac{(X_2^2 - X_1 X_3 - Gr_t X_4 - Gr_s X_6 + M X_2)}{\left(\frac{\mu_{nf}}{\rho_{nf} \nu_{bf}} \left(1 + \frac{1}{\gamma} \right) \right)} \quad (22)$$

$$X'_4 = X_5, \quad (23)$$

$$\begin{aligned} X'_5 &= -\frac{Pr X_1 X_5}{A_1} - \frac{N_b X_5 X_7}{A_1} - \frac{N_t X_5^2}{A_1} \\ &+ \frac{\mu_{nf}}{\rho_{nf} \nu_{bf} A_1} Pr Ec X_3^2 + \frac{Pr ME c X_2^2}{A_1} \end{aligned} \quad (24)$$

$$X'_6 = X_7, \quad (25)$$

$$X'_7 = -Sc X_1 X_7 - \frac{N_t}{N_b} X'_6. \quad (26)$$

with the initial and boundary conditions

$$\begin{aligned} X_1(0) &= 0, X_2(0) = 1, X_5(0) = Bi(X_4(0) - 1), X_6(0) = 0 \\ X_2(\infty) &\rightarrow 0, X_4(\infty) \rightarrow 0, X_6(\infty) \rightarrow 0. \end{aligned} \quad (27)$$

The boundary conditions are converted to initial conditions

$$\begin{aligned} X_1(0) &= 0, X_2(0) = 1, X_3(0) = s_1, X_4(0) = 0, \\ X_5(0) &= s_2, X_6(0) = 0, X_7(0) = s_3. \end{aligned} \quad (28)$$

and s_1, s_2 and s_3 are obtained using Shooting Technique to ensure that

$$X_5(0) = Bi(X_4(0) - 1), X_2(\infty) \rightarrow 0, X_4(\infty) \rightarrow 1 \quad (29)$$

are satisfied.

3.2. Numerical Method

The resulting system of ODEs are solved numerically using the Runge-Kutta-Gills method. The Runge-Kutta scheme of the fourth order for the first order ordinary differential equation

$$y' = f(x, y) \quad (30)$$

is given as

$$y_{n+1} = y_n + \frac{1}{6}(K_1 + 2K_2 + 2K_3 + K_4) \quad (31)$$

$$K_1 = hf(x_n, y_n), \quad (32)$$

$$K_2 = hf\left(x_n + \frac{h}{2}, y_n + \frac{1}{2}K_1\right), \quad (33)$$

$$K_3 = hf\left(x_n + \frac{h}{2}, y_n + \frac{1}{2}K_2\right), \quad (34)$$

$$K_4 = hf(x_n + h, y_n + K_3). \quad (35)$$

The Runge-Kutta-Gills scheme is a modification of the Runge-Kutta scheme which is stable for $h \leq \frac{2.8}{\lambda}$ and it is given as

$$y_{n+1} = y_n + \frac{1}{6}(K_1 + 2bK_2 + 2dK_3 + K_4) \quad (36)$$

$$K_1 = hf(x_n, y_n), \quad (37)$$

$$K_2 = hf\left(x_n + \frac{h}{2}, y_n + \frac{1}{2}K_1\right), \quad (38)$$

$$K_3 = hf\left(x_n + \frac{h}{2}, y_n + aK_1 + bK_2\right), \quad (39)$$

$$K_4 = hf(x_n + h, y_n + cK_2 + dK_3), \quad (40)$$

with constants chosen as

$$a = \frac{\sqrt{2}-1}{2}, b = \frac{2-\sqrt{2}}{2}, c = \frac{\sqrt{2}}{2}, d = \frac{2+\sqrt{2}}{2}. \quad (41)$$

4. Discussion of Results

The flow of electrically conducting nanofluid made from Engine oil as base fluid and Copper *Cu* nanoparticle over a convectively heated vertical surface is studied herewith. See table 1 for the thermophysical properties of the base fluid and the nanoparticles. Unless otherwise stated, the values of the parameters used are $\gamma = 1$; $Gr_t = 1$; $Gr_s = 3$; $M = 3$; $Pr = 7.62$; $Ec = 0.1$; $\phi = 0.01$; $N_t = 0.1$; $N_b = 0.1$; $Sc = 0.62$; $Bi = 0.1$.

Table 1. Thermophysical properties of Engine oil and nanoparticles.

Material	ρ (kg/m ³)	c_p (J/kgK)	k (W/mk)	β (K ⁻¹)	σ (S/m)
Engine oil	804	1909	0.145	70×10^{-5}	1.00×10^{-7}
Copper (<i>Cu</i>)	8933	385	401	1.67×10^{-5}	5.96×10^7

The magnetic field applied normal to the direction of fluid flow induces the Lorentz force which inhibits fluid motion. This is revealed in Figure 2 where the primary velocity reduces with increasing magnetic field strength. This result corroborates the findings in Ahmad et al. [1, 2], Bulinda et al. [3], Chen et al. [4], and Farooq et al. [5]. The internal friction generated from the reduced velocity produces more heat energy and thereby increases the temperature of the flow as shown in figure 3 and the finding here agrees with the findings in Ahmad et al. [1], Bulinda et al. [3], and Farooq et al. [5]. Biot number is the ratio of internal resistance to conduction to the resistance of flow to convective heat transfer. As the resistance to conductive heat transfer increases, flow temperature increases and this is as seen in figure 4. The flow tends to a Newtonian flow as Casson parameter γ increases and flow properties are inhibited. Hence, the flow temperature and flow velocity reduce as $\gamma \rightarrow \infty$ and this is depicted in figures 5 and 6. The effects of the Casson fluid parameter observed in this study also agrees with the results in Kataria and Patel [9], Mustafa and Khan [16], Mutuku [17], and Pramanik [25].

An increase in Eckert number leads to an increase in the flow velocity and flow temperature (see figures 7 and 8). Meanwhile increase in the nanoparticle volume fraction leads to quick sedimentation of the nanoparticles at the wall surface, thereby inhibiting flow flow and heat transfer. This is evident in figures 9 and 10 where the flow velocity and flow temperature decreases as ϕ increases.

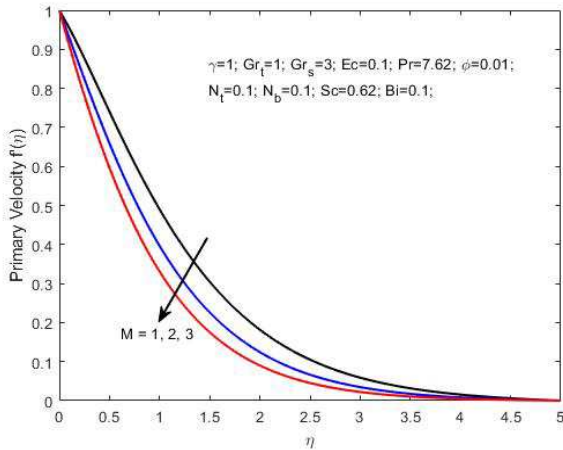


Figure 2. Variation of primary velocity with magnetic field strength.

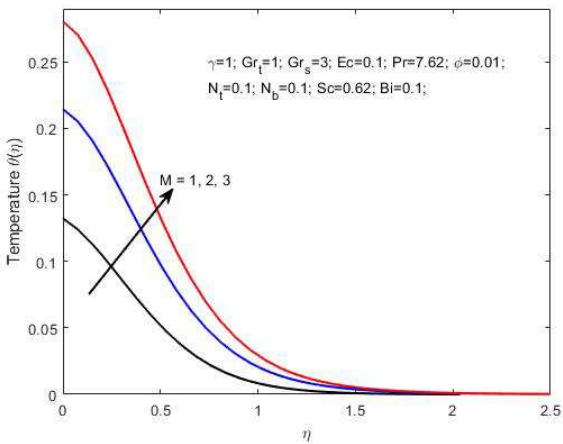


Figure 3. Variation of temperature with magnetic field strength.

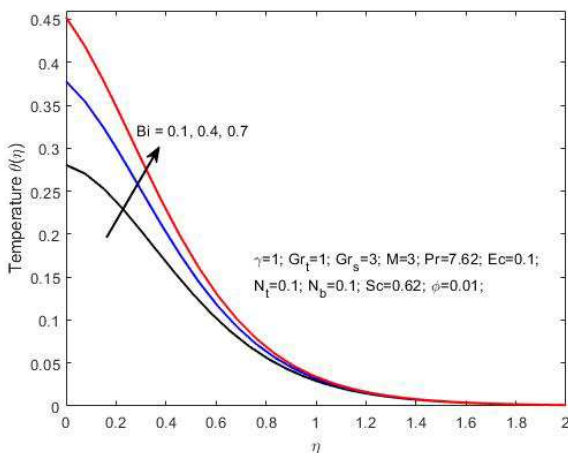


Figure 4. Variation of temperature with Biot number.

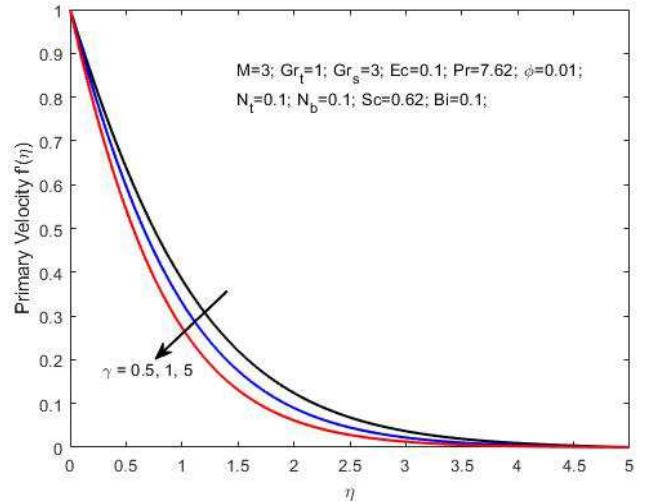


Figure 5. Variation of primary velocity with Casson fluid parameter.

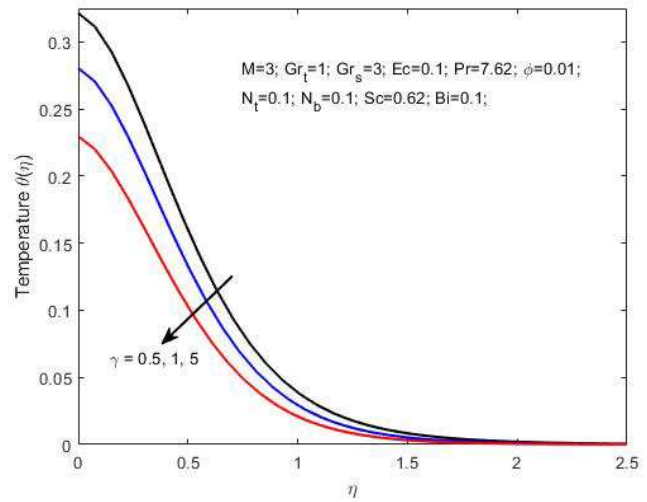


Figure 6. Variation of temperature with Casson fluid parameter.

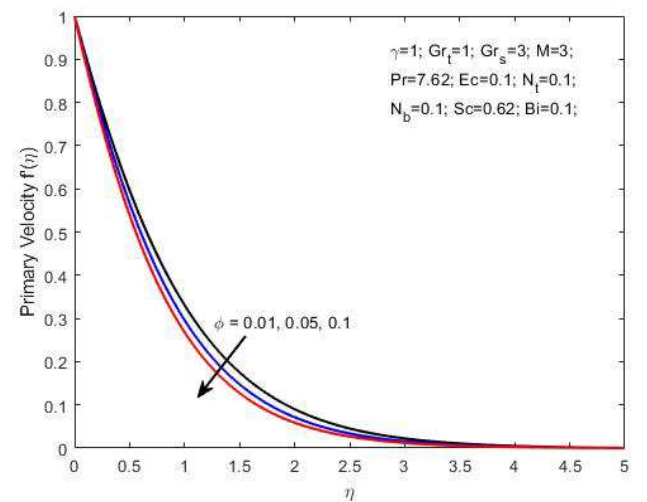


Figure 7. Variation of primary velocity with nanoparticle volume fraction.

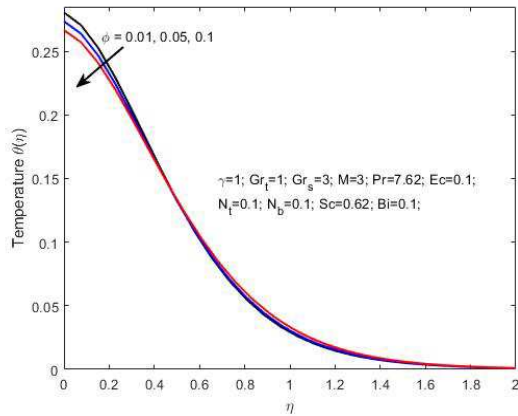


Figure 8. Variation of temperature with nanoparticle volume fraction.

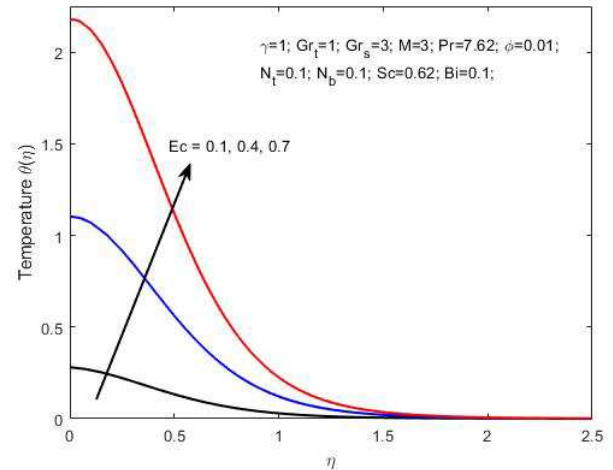


Figure 10. Variation of temperature with Eckert number.

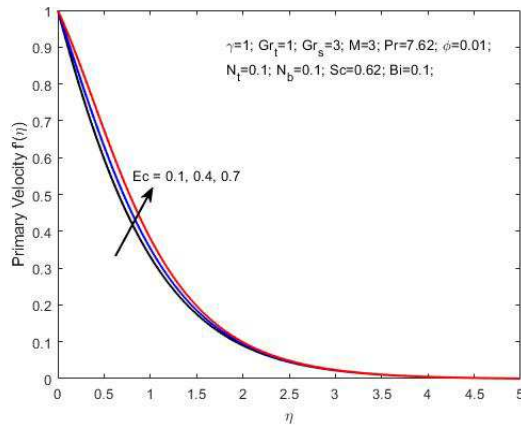


Figure 9. Variation of primary velocity with Eckert number.

5. Conclusion

In this study, a magnetohydrodynamic flow of Casson nanofluid over a vertical plate is analysed. It is found out that;

1. Increasing magnetic field increases flow temperature but decreases flow velocity.
2. Increasing Casson parameter leads to a decrease in both flow temperature and velocity
3. Increase in Eckert number leads to an increase the flow velocity and flow temperature.
4. increase in the nanoparticle volume fraction leads to a decrease in both flow velocity and flow temperature.

Nomenclature

T	Temperature	u, v	velocity components in the x, y - directions
c_p	Specific heat capacity	C	Concentration of nanoparticle
n	Velocity index	g	Acceleration due to gravity
B_0	magnetic field strength	μ	Coefficient of dynamic viscosity
σ	electrical conductivity	β_T, β_C	coefficient of thermal and concentration expansion
γ	Casson fluid parameter	D_B, D_T	Brownian and thermophoretic diffusion coefficient
κ	thermal conductivity	T_w, T_∞	Wall and free stream temperature
α	thermal diffusivity	C_w, C_∞	Wall and free stream concentration
ρ	fluid density	ϕ	nanoparticle volume fraction
Ec	Eckert number	Gr_t, Gr_s	Thermal and Solutal Grashof parameter
M	Magnetic field parameter	Pr	Prandtl number
Sc	Schmidt number	N_b, N_t	Brownian and thermophoretic parameter

Subscripts

nf	Nanofluid	np	nanoparticle	bf	base fluid
------	-----------	------	--------------	------	------------

References

- [1] Ahmad, I., Sajid, M., Awan, W., Rafique, M., Aziz, W., Ahmed, M., Abbasi, A., and Taj, M. (2014). MHD flow of a viscous fluid over an exponentially stretching sheet in a porous medium. *Journal of Applied Mathematics*, 2014: 256761.
- [2] Ahmad, S., Yousaf, M., Khan, A., and Zaman, G. (2018). Magnetohydrodynamic fluid flow and heat transfer over a shrinking sheet under the influence of thermal slip. *Heliyon*, 4 (30364604): e00828–e00828.
- [3] Bulinda, V. M., Kangethe, G. P., and Kiogora, P. R. (2020). Magnetohydrodynamics free convection flow of incompressible fluids over corrugated vibrating bottom surface with hall currents and heat and mass transfers. *Journal of Applied Mathematics*, 2020: 2589760.

- [4] Chen, W. Z., Yang, Q. S., Dai, M. Q., and Cheng, S. M. (1998). An analytical solution of the heat transfer process during contact melting of phase change material inside a horizontal elliptical tube. *International Journal of Energy Research*, 22 (2): 131–140.
- [5] Farooq, U., Lu, D., Munir, S., Ramzan, M., Suleman, M., and Hussain, S. (2019). MHD flow of Maxwell fluid with nanomaterials due to an exponentially stretching surface. *Scientific Reports*, 9 (1): 7312.
- [6] Gbadeyan, J. A., Titiloye, E. O., and Adeosun, A. T. (2020). Effect of variable thermal conductivity and viscosity on Casson nanofluid flow with convective heating and velocity slip. *Heliyon*, 6: e03076.
- [7] Idowu, A. S., Akolade, M. T., Abubakar, J. U., and Falodun, B. O. (2020). MHD free convective heat and mass transfer flow of dissipative Casson fluid with variable viscosity and thermal conductivity effects. *Journal of Taibah University for Science*.
- [8] Jabeen, K., Mushtaq, M., and Akram, R. M. (2020). Analysis of the MHD boundary layer flow over a nonlinear stretching sheet in a porous medium using semianalytical approaches. *Mathematical Problems in Engineering*, 2020: 3012854.
- [9] Kataria, H. R. and Patel, H. R. (2018). Heat and mass transfer in magnetohydrodynamic (MHD) Casson fluid flow past over an oscillating vertical plate embedded in porous medium with ramped wall temperature. *Propulsion and Power Research*, 7 (3): 257–267.
- [10] Kolenko, T., Glogovac, B., and Jaklic, T. (1999). An analysis of a heat transfer model for situations involving gas and surface radiative heat transfer. *Communications in Numerical Methods in Engineering*, 15 (5): 349–365.
- [11] O. K. Koriko, K. S. Adegbe, A. S. Oke, I. L. Animasaun, (2020). Exploration of Coriolis force on motion of air over the upper horizontal surface of a paraboloid of revolution, *Phys. Scr.* 95 (3) (2020) 035210, doi: 10.1088/1402-4896/ab4c50.
- [12] O. K. Koriko, K. S. Adegbe, A. S. Oke, I. L. Animasaun, (2020a) Corrigendum: exploration of Coriolis force on motion of air over the upper horizontal surface of a paraboloid of revolution, (2020 *Phys. Scr.* 95 035210), *Physica Scripta* 95 (11) (2020) 119501, doi: 10.1088/1402-4896/abc19e.
- [13] Kumar, B. V. R., Murthy, P. V. S. N., and Singh, P. (1998). Free convection heat transfer from an isothermal wavy surface in a porous enclosure. *Int. J. Numer. Meth. Fluids*, 28: 633–661.
- [14] Mahantesh, N. M., Kemparaju, M. C., and Raveendra, N. (2020). Double-diffusive free convective flow of Casson fluid due to a moving vertical plate with non-linear thermal radiation. *World Journal of Engineering*, 14 (1): 851–862.
- [15] Maiga, S. E. B., Nguyen, C. T., Galanis, N., and Roy, G. (2004). Heat transfer behaviours of nanofluids in a uniformly heated tube. *Superlattices Microstructures*, 35: 543–557.
- [16] Mustafa, M. and Khan, J. A. (2015). Model for flow of Casson nanofluid past a non-linearly stretching sheet considering magnetic field effects. *AIP Advances*, 5 (077148).
- [17] Mutuku, W. N. (2016). Ethylene glycol (EG)-based nanofluids as a coolant for automotive radiator. *Asia Pac. J. Comput. Engin.* 3 (1).
- [18] Mutuku-Njane, W. N. and Makinde, O. D. (2013). Combined effect of buoyancy force and Navier slip on MHD flow of a nanofluid over a convectively heated vertical porous plate. *The Scientific World Journal* Volume, Article ID 725643, 2013.
- [19] Nadeem, S., Haq, R. U., Akbar, N. S., and Khan, Z. H. (2013). MHD three-dimensional Casson fluid flow past a porous linearly stretching sheet. *Alexandria Engineering Journal*, 52 (4): 577–582.
- [20] A. S. Oke, W. N. Mutuku, M. Kimathi, I. L. Animasaun, (2020) Insight into the dynamics of non-Newtonian Casson fluid over a rotating non-uniform surface subject to Coriolis force, *Nonlinear Eng.* 9 (1) (2020) 398–411, doi: 10.1515/nleng-2020-0025.
- [21] A. S. Oke, W. N. Mutuku, M. Kimathi, I. L. Animasaun, (2020a) Coriolis effects on MHD Newtonian flow over a rotating non-uniform surface, *Proc. Inst. Mech. Eng., Part C: J. Mech. Eng. Sci. (PIC)*, in-press (2020a), doi: 10.1177/0954406220969730.
- [22] A. S. Oke, I. L. Animasaun, W. N. Mutuku, M. Kimathi, Nehad Ali Shah, S. Saleem, (2021) Significance of Coriolis force, volume fraction, and heat source/sink on the dynamics of water conveying 47 nm alumina nanoparticles over a uniform surface, *Chinese Journal of Physics*, 2021, ISSN 0577-9073, doi: 10.1016/j.cjph.2021.02.005.
- [23] Pak, B. C. and Cho, Y. I. (1998). Hydrodynamic and heat transfer study of dispersed fluids with submicron metallic oxide particles. *Experimental Heat Transfer: A Journal of Thermal Energy Generation, Transport, Storage, and Conversion*, 11 (2): 151–170.
- [24] Piechowski, M. (1998). Heat and mass transfer model of a ground heat exchanger: validation and sensitivity analysis. *International Journal of Energy Research*, 22 (11): 965–979.
- [25] Pramanik, S. (2014). Casson fluid flow and heat transfer past an exponentially porous stretching surface in presence of thermal radiation. *Ain Shams Engineering Journal*, 5 (1): 205–212.
- [26] Saadatian, E., Lam, R., and Mota, J. P. B. (1999). Natural convection heat transfer in the annular region between porous confocal ellipses. *International Journal for Numerical Methods in Fluids*, 31 (2): 513–522.
- [27] Shah, Z., Kumam, P., and Deebani, W. (2020). Radiative MHD Casson nanofluid flow with activation energy and chemical reaction over past nonlinearly stretching surface through entropy generation. *Scientific Reports*, 10 (1): 4402.
- [28] Venkateswarlu, S., K., V. S. V., and Durga, P. P. (2020). MHD flow of MoS₂ and MgO water based nanofluid through porous medium over a stretching surface with cattaneo-christov heat flux model and convective boundary condition. *International Journal of Ambient Energy*, 0 (0): 1–10.
- [29] Wasp, F. J. (1977). Solid-liquid flow slurry pipeline transportation. *Trans. Tech. Pub., Berlin*.
- [30] Xuan, Y. and Roetzel, W. (2000). Conceptions for heat transfer correlation of nanofluids. *International Journal of Heat and Mass Transfer*, 43 (19): 3701–3707.
- [31] Yang, Y.-T., Chen, C.-K., and Chi-Fang (1996). Convective heat transfer from a circular cylinder under the effect of a solid plane wall. *International Journal for Numerical Methods in Fluids*, 23 (2): 163–176.

- [32] Zerroukat, M., Power, H., and Chen, C. S. (1998). A numerical method for heat transfer problems using collocation and radial basis functions. *International Journal for Numerical Methods in Engineering*, 42 (7): 1263–1278.